

Detection of Low Adhesion in the Railway Vehicle Wheel/Rail Interface: Assessment of Multi-Bodied Simulation Data

Christopher Ward, Roger Goodall, Roger Dixon
School of Electronic, Electrical
and Systems Engineering
Loughborough University
Loughborough, Leicestershire
UK, LE11 3TU
Email: c.p.ward@lboro.ac.uk, r.m.goodall@lboro.ac.uk,
r.dixon@lboro.ac.uk

Guy Charles
Faculty of Engineering
Coates Building
University of Nottingham
Nottingham
UK, NG7 2RD
Email: guy.charles@nottingham.ac.uk

Abstract—Low adhesion in the wheel/rail interface of railway vehicles creates safety and punctuality issues in terms of missed station stops and signals passed at danger. RSSB project T959 is tasked with developing advanced monitoring techniques for the detection of adhesion in this key interface. A number of techniques were developed and initially tested on simplified models of a rail vehicle. The efficacy of these techniques is now being tested with more representative data produced by multi-bodied physics simulation package Vampire. This paper therefore covers the outcomes of the Vampire testing, initial application of a Kalman-Bucy filter creep force estimator to the Vampire data, and application of a data comparison method based upon the Sprague and Geers method, also to the Vampire data.

I. INTRODUCTION

Low adhesion in the wheel/rail contact of railway vehicles is a current issue occupying the railway industry. This is commonly reported as the ‘leaves on the line’ issue and can create large safety and punctuality issues as rail vehicles fail to stop at stations or pass signals at danger. RSSB managed project T959 [7] is tasked with finding methods of estimating the available adhesion in the wheel/rail interface using modest cost vehicle-mounted sensor sets and advanced filtering applied to in-service vehicles. Knowledge of this would allow numerous commercial benefits such as targeting mitigation methods more efficiently and scheduling rail services to make best potential use of the available adhesion.

Early stages of project T959 investigated a number of low adhesion estimation techniques as applied to simplified plan view dynamics models of typical railway vehicles and were highlighted in [9]. The primary amongst these methods was application of a Kalman-Bucy filter (KBF) [3] which was used to estimate creep forces (longitudinal and lateral forces arising from contact mechanics of the wheel-rail interface), that were then post-processed to imply an adhesion level. Additional techniques were multiple/interacting Kalman filters and data comparison techniques. The efficacy of these methods is now being tested on more representative data produced through

a multi-bodied simulation (MBS) package Vampire, success of which will lead to full scale physical testing on a fully instrumented rail vehicle.

This paper therefore covers: brief outcomes of the Vampire simulations and how these compare to the MATLAB/Simulink modelling; initial application of the KBF technique and current issues; and finally a data driven method of non-model based comparison currently being developed using the Sprague and Geers metric [8].

II. VAMPIRE MULTI-BODIED SIMULATION

The current phase of the project is using data produced by the MBS package Vampire, [1]. The data produced from the package includes the full nonlinearity of the suspension system, as well as the nonlinearity in the wheel/rail contact. It also encapsulates any interaction of the vertical suspension components with the lateral and yaw suspension.

A. Vehicle selection

The vehicle selected for testing is the British Rail Mk.3 coach. This vehicle was selected due to: vehicle models being readily available; and the physical testing will be likely to take place with this vehicle.

Parameters were interpreted from the MBS model to fit with the simpler plan view lateral and yaw models used for the filter design (Figure 1(a) for the primary suspension and Figure 1(b) for the secondary suspension, with parameter values shown in Table I). The Mk.3 coach is an older form of coach with many features than are no longer incorporated in vehicle design. In particular the secondary yaw damper (that increases the critical speed of bogie instability [11]) is a friction damper rather than the more common viscous damper. Due to the discontinuous nature of this component it adds a significant nonlinearity to the system that cannot be incorporated easily in a state space model.

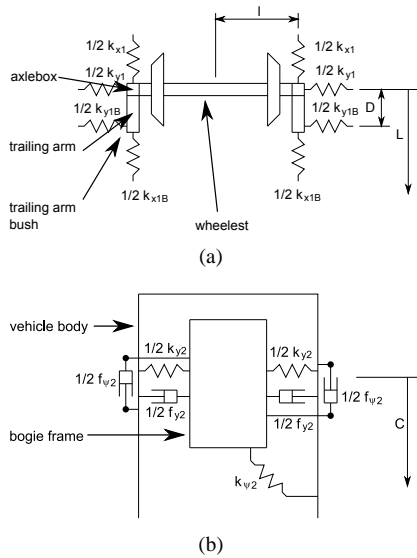


Fig. 1. Suspension layouts, (a) primary suspension, (b) secondary suspension

Parameter	Symbol	Value	Units
Body mass	m_v	24380	kg
Body yaw inertia	I_v	1129740	kgm ²
Bogie mass	m_b	2130	kg
Bogie yaw inertia	I_b	2870	kgm ²
Wheelset mass	m_w	1475	kg
Wheelset yaw inertia	I_w	910	kgm ²
Nominal radius	r_0	0.4570	m
Lateral stiffness (2nd)	k_{y2}	197000	N/m
Lateral damping (2nd)	f_{y2}	40000	Ns/m
Yaw stiffness (2nd)	$k_{\psi 2}$	175000	Nm
Yaw damper friction breakout (2nd)	$f_{\psi 2}$	11860	N
Longitudinal stiffness (1st)	k_{x1}	204800	N/m
Lateral stiffness (1st)	k_{y1}	204800	N/m
Longitudinal damping (1st)	f_{x1}	0	Ns/m
Lateral damping (1st)	f_{y1}	0	Ns/m
Longitudinal stiffness, bush (1st)	k_{x1b}	15696000	N/m
Lateral stiffness, bush (1st)	k_{y1b}	15456000	N/m
Longitudinal damping, bush (1st)	f_{x1b}	19400	Ns/m
Lateral damping, bush (1st)	f_{y1b}	13200	Ns/m

TABLE I
MK.3 COACH INTERPRETED PARAMETERS

B. Wheel/rail contact adhesion conditions and test runs

As highlighted in [9] the shape of the creep curves is critical to the detection of areas of low adhesion. It is assumed that the initial slope of the creep curve is constant for all adhesion conditions and that the differentiating factor is the level of creep saturation, [2]. However, as first highlighted in [5] and subsequently verified using the University of Sheffield SUROS twin-disk machine [10], the initial slope of the creep curve reduces as the adhesion conditions reduce, meaning changes in adhesion can be determined in ‘normal’ running and not just when the contact forces are saturated. Therefore four adhesion condition creep curves were set at dry, wet, low and very low levels for the Vampire simulation testing, Figure 2. These can be thought of as relating to friction coefficients of 0.56, 0.32, 0.072 and 0.038 respectively.

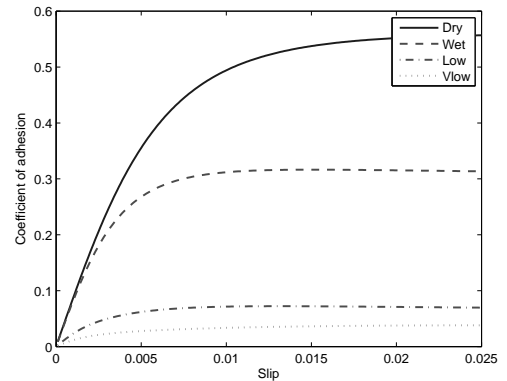


Fig. 2. Creep curves developed from the University of Sheffield SUROS twin disk machine

As with any such form of simulation there are a huge number of potential test combinations. The available variables were narrowed down to: track conditions (straight line, 200 km/h design speed); vehicle speed (100 km/h and 200 km/h); track irregularity sizes (full scale and half scale); and adhesion levels (constant, step changes and continuously varying).

C. Vampire modelling observations

MATLAB/Simulink modelling in [9] demonstrated that the creep forces in the wheel/rail contact reduce as the adhesion level reduces. This trend is repeated with the Vampire simulation, Figure 3(a), for the lateral creep forces of the front wheelset of the front bogie. These tests were performed at a vehicle speed of 200 km/h and with full sized track irregularity where there is a drop in the RMS of the lateral creep force from 1340 N for the dry adhesion case to 300 N for the very low adhesion case. However in the lateral case there is a constant ‘gravitational’ stiffness force that arises from the profiling of the wheel and varies little with adhesion conditions. This has an RMS value of 1300 N, therefore masking changes in the creep forces when estimated in combination. The creep moment demonstrates an even larger change in RMS between the dry adhesion case, 2900 Nm, and the very low adhesion case, 310 Nm, shown in Figure 3(b). Here gravitational moment is negligible.

III. CREEP FORCE ESTIMATION

The KBF method of creep force estimation uses a simplified full vehicle model or half vehicle model. The latter approach is favourable due to potential reduction in sensors required and associated reduced order of the model.

A. Open loop model comparison, half vehicle model

The open loop estimator model is first validated against the Vampire simulation outputs. The creep force estimator model is output only and does not include any terms from the track irregularity that would be costly to measure in practice. In order to test the open loop estimator model the

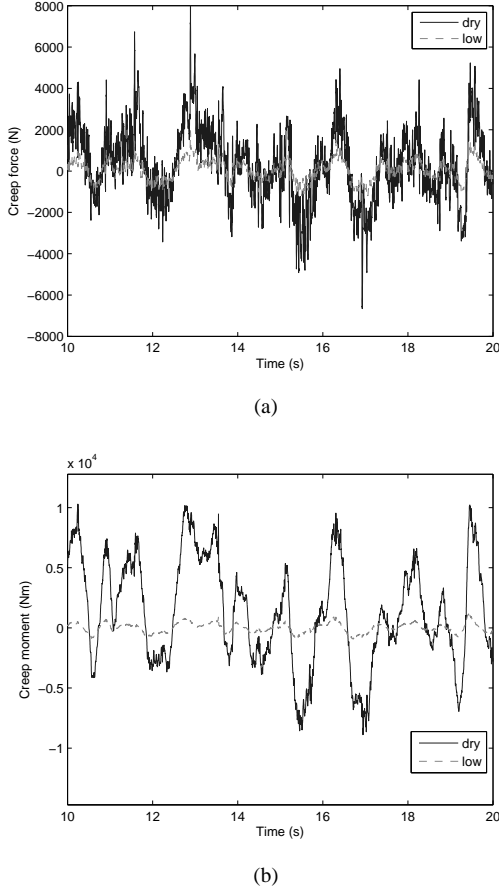


Fig. 3. Vampire modelling creep reductions, (a) lateral, (b) yaw

state space format is subtly modified to include the track irregularities as generated by the Vampire simulation model. The suspension models are linear formations and follow the simplified suspension layouts of Figures 1(a) and 1(b). The lateral and yaw dynamic equations of each wheelset are

$$m_w \ddot{y}_w = F_s + F_g + F_c \quad (1)$$

$$I_w \ddot{\psi}_w = M_s + M_g + M_c \quad (2)$$

where m_w is the mass of the wheelset, \ddot{y}_w is the lateral acceleration of the wheelset, F_s is the lateral primary suspension forces, F_g is the lateral gravitational stiffness, F_c is the lateral creep force, I_w is the moment of inertia of the wheelset, $\ddot{\psi}_w$ is the yaw acceleration of the wheelset, M_s is the primary suspension yaw moment, M_g is the gravitational moment and M_c is the creep moment. For this linear estimator model, the open loop tests use the creep forces and moments of Kalker [2]

$$F_c = 2f_{22}\psi_w - \frac{2f_{22}}{V}\dot{y}_w \quad (3)$$

$$M_c = -\frac{2l\lambda f_{11}}{r_0}(y_w - d_r) - \frac{2l^2 f_{11}}{V}\dot{\psi}_w \quad (4)$$

where f_{11} is the longitudinal creep coefficient (5770000 N for the dry adhesion case, and 339000 N for the very low

Gain	Phase	R^2	Gain	Phase	Combined
0.5	0	0.75	-0.5	0	0.5
1	0	1	0	0	0
2	0	0	1	0	1
1	-90	-1.09	0	0.52	0.52
1	90	-0.86	0	0.48	0.48
1	180	-3	0	1	1

TABLE II
SPRAGUE AND GEERS METRIC TEST

adhesion case), f_{22} is the lateral creep coefficient (5770000 N for the dry adhesion case, and 339000 N for the very low adhesion case), V is the vehicle speed (200 km/h), λ is wheelset conicity (0.131) and d_r is rail lateral irregularity.

Figure 4(a) shows a section of half vehicle open loop model data excited by the track irregularity file compared to the Vampire outputs for the dry adhesion case for the front wheelset yaw, yaw rate and yaw accelerations. Visual inspection shows some differences between the outputs in terms of gain, but that the general trend is that the frequency content is followed. Numerically this is assessed using the Sprague and Geers metric.

1) *Sprague and Geers metric*: This metric was initially used for the comparison of different wave patterns in fluid flows. If $m(t)$ is the measured history and $c(t)$ is the estimated history, then a number of time integrals can be defined

$$v_{mm} = (t_2 - t_1)^{-1} \int_{t_1}^{t_2} m^2(t) dt \quad (5)$$

$$v_{cc} = (t_2 - t_1)^{-1} \int_{t_1}^{t_2} c^2(t) dt \quad (6)$$

$$v_{mc} = (t_2 - t_1)^{-1} \int_{t_1}^{t_2} m(t)c(t) dt \quad (7)$$

where $t_1 < t < t_2$ is the time step of interest, the error in the magnitude is given as

$$M_{SG} = \sqrt{\frac{v_{cc}}{v_{mm}}} - 1 \quad (8)$$

the phase error is given by

$$P_{SG} = \frac{1}{\pi} \cos^{-1} \left(\frac{v_{mc}}{\sqrt{v_{mm}v_{cc}}} \right) \quad (9)$$

these two errors can be combined to give an overall global error

$$C_{SG} = \sqrt{M_{SG}^2 + P_{SG}^2} \quad (10)$$

this is comparable to the R^2 method of [4], but is able to cope with a degree of phase lag in the signals. This is illustrated in Table II for a series of sine wave comparison tests where the wave is scaled and phased. This demonstrates that the Sprague and Geers Metric can give information about the size and direction of the gain comparison between the original and estimated value, whereas the R^2 metric begins to fail when the scaling is past 2. The Sprague and Geers metric also gives good metrics information when there is phase difference

between the signals as will be the case in this application where the signals may not be perfectly aligned, under which conditions the R^2 metric fails to see a correlation.

The Sprague and Geers metrics for the open loop model correlation are summarised in Table III. These values show for the acceleration and position signals that they are approximately 1.2 times larger than those from Vampire and the rate signal is 1.5 times larger. There is also mainly agreement in the phase signals of the analysis, with phases of less than 40° , though this is more difficult to interpret with more widely spaced spectrum signals. The modelling gives some confidence that the robust properties of the KBF would be able to accommodate model mismatches of this order. Figure 4(b) shows a section of open loop and Vampire output data for the very low adhesion case. This shows that the open loop model now is no longer correlated with the Vampire data, either in terms of gain or phase. This is reflected in the Sprague and Geers metrics shown in Table III, where the phase equivalent is considerably larger for the dry case and gain content is mostly much lower than that observed from the Vampire simulation with the exception of the yaw angle.

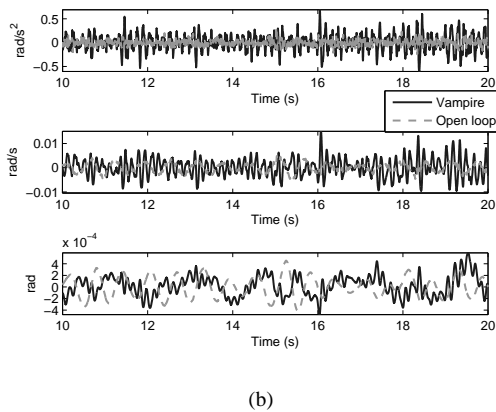
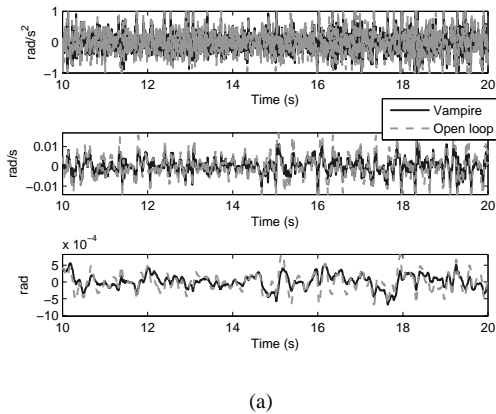


Fig. 4. Open loop estimator model comparison with Vampire output data, (a) dry case, (b) very low

This therefore represents a significant model mismatch at

Condition	Parameter	Gain	Phase	Combined
Dry	$\dot{\psi}_{FF}$	0.1971	0.1332	0.2379
Dry	ψ_{FF}	0.5727	0.1528	0.5928
Dry	ψ_{FF}	0.1990	0.2497	0.3193
Very low	$\dot{\psi}_{FF}$	-0.5923	0.4922	0.7701
Very low	ψ_{FF}	-0.4603	0.5585	0.7238
Very low	ψ_{FF}	-0.0390	0.5730	0.5744

TABLE III
SPRAGUE AND GEERS METRIC COMPARISONS FOR THE OPEN LOOP ESTIMATOR MODEL

the lower adhesion levels and may be due to a number of reasons that have not full been understood: stick/slip dynamics in the the secondary yaw damper of the vehicle body and bogie, poor model extraction from the Vampire modelling, etc. Steps are currently being undertaken to understand these dynamics.

B. Creep force estimation example

The open loop suspension modelling from the previous section is now applied to the KBF creep force estimation method. It is noted at the outset that due to the discrepancies in the estimator modelling of the Mk.3 coach at low adhesion levels it is expected that the KBF performance will be affected. The size of this performance deficit requires assessment due to the robust qualities of the KBF.

For this example a full possible measurement vector is used

$$y = [y_{FF} \dot{y}_{FF} \psi_{FF} \dot{\psi}_{FF} y_{FR} \dot{y}_{FR} \dots \dots \psi_{FR} \dot{\psi}_{FR} y_{BF} \dot{y}_{BF} \psi_{BF} \dot{\psi}_{BF} \dots \dots y_V \dot{y}_V]^T \quad (11)$$

where the subscript FF refers to the front wheelset of the front bogie, subscript FR refers to the rear wheelset of the front bogie, subscript BF refers to the front bogie and subscript V refers to the vehicle body. It should be noted that this case represents the highest number of measurements possible and will not be practical in a long term application. The state vector is defined as

$$x = [y_{FF} \dot{y}_{FF} \psi_{FF} \dot{\psi}_{FF} y_{FR} \dot{y}_{FR} \dots \dots \psi_{FR} \dot{\psi}_{FR} y_{BF} \dot{y}_{BF} \psi_{BF} \dot{\psi}_{BF} \dots \dots y_V \dot{y}_V F_{FF} F_{FR} M_{FF} M_{FR}]^T \quad (12)$$

where F is the lateral creep force and gravitational stiffness combined, and M is the combined gravitational and creep moment. No physics of the creep forces are included in the estimator model, instead this is defined as

$$\dot{F}_{FF} = \dot{F}_{FR} = \dot{M}_{FF} = \dot{M}_{FR} = 0 \quad (13)$$

The Q and R covariance matrices were selected heuristically through multiple iterations. The Q matrix essentially defines that the state matrix has a high level certainty for the wheelset models, with less certainty assigned to the bogie and vehicle dynamics due to the use of a half vehicle estimator model. The creep force and moment sections are assigned the

highest level uncertainty due to the assumptions of Equation 13, where

$$Q = \text{diag}[1e^{-10}, 1e^{-10}, 1e^{-10}, 1e^{-10}, 1e^{-10}, 1e^{-10}, \dots, \dots, 1e^{-10}, 1e^{-10}, 1e^5, 1e^5, 1e^{10}, 1e^{10}, \dots, \dots, 1e^5, 1e^5, 1e^{20}, 1e^{20}, 1e^{20}, 1e^{20}] \quad (14)$$

The measurement covariance R is defined as

$$R = \text{diag}[1e^{-3}, 1, 1e^{-3}, 1, 1e^{-3}, 1, 1e^{-3}, \dots, \dots, 1, 1e^5, 1e^5, 1e^5, 1e^5, 1e^{10}, 1e^{10}] \quad (15)$$

where the wheelset measurement are scaled in relation to their variance. The bogie and vehicle measurements are again treated as a higher level uncertainty due to the use of a half vehicle estimator.

Figure 5(a) shows an example of the creep moment estimation for the front wheelset of the front bogie at the dry adhesion level. Visual inspection shows that the estimator is identifying the correct frequency content of the creep moment but is over estimating the gain of the signal. This is reinforced by the Sprague and Geers metric of the estimation shown in Table IV.

As with the open loop estimator the KBF estimator shows poor convergence to the creep moment of the front wheelset of the front bogie at the very low adhesion level, Figure 5(b). The KBF in this case has failed to account for any discrepancies in the modelling. This is again reinforced by the poor values provided by the Sprague and Geers metric in Table IV.

Condition	Parameter	Gain	Phase	Combined
Dry	M_{FF}	0.8671	0.2493	0.9023
Very low	M_{FF}	6.5419	0.3912	6.5536

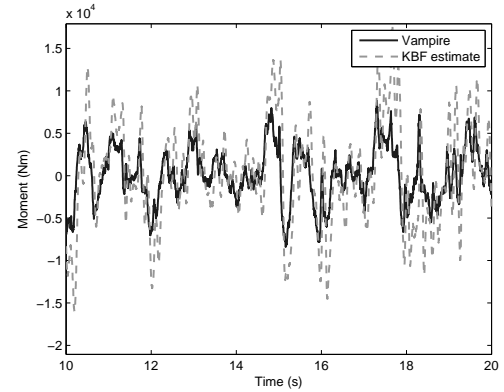
TABLE IV
CREEP MOMENT ESTIMATION SPRAGUE AND GEERS METRIC

C. Development areas

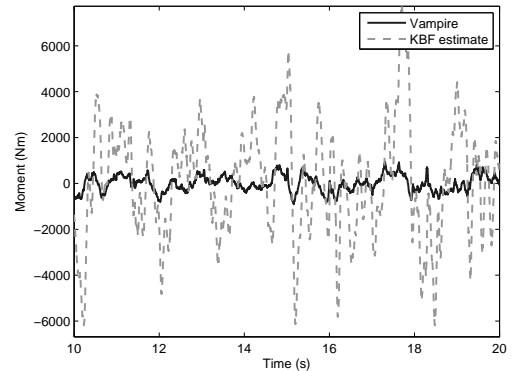
There are clearly discrepancies between the modelling as performed in the MATLAB/Simulink phase of the project and the Vampire simulation package. Currently work is on-going to determine the cause of these differences as it is still hoped that the creep force estimation method of low adhesion estimation offers a high performance and robust solutions once these initial issues are rectified.

IV. NON-MODEL BASED COMPARISON TECHNIQUE

An alternative method to the model based KBF creep force estimation of the previous section and as proposed in [9] is the use of known adhesion level ‘training’ data sets and real time advanced comparison computational methods. The basic concept of the idea is shown in Figure 6, that of comparing data gathered when the adhesion levels are considered acceptable and comparing this to the current measured data to determine any changes. This method’s success rests upon a number of factors: that the vehicle being tested runs at consistent speed profile down the same section of track on numerous occasions



(a)



(b)

Fig. 5. KBF estimation of the creep moment using a half vehicle estimator for the front wheelset of the front bogie, (a) dry case, (b) very low

(ideal for service vehicles); that the system excitation (the track irregularity) doesn’t vary too greatly with time; and that spatial data can be stored and recalled in an efficient and accurate manner. The advantage with this type of system is that the processing requirements are much reduced and the limiting computational factor is now essentially one of storage.

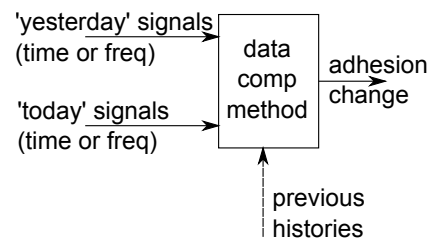


Fig. 6. Sensor signal comparison method

The processing algorithm used is the Sprague and Geers metric, [8]. In this simple demonstration of the method, the signal from an simulated lateral accelerometer mounted on the front bogie frame away from the centre of mass is used. Mounting on the bogie rather than the wheelset is much

more advantageous due to the large accelerations ($\pm 300 g$) experienced at the wheelset level. A resolution adequate for the application is assumed and the sample rate is 100 Hz.

A. Threshold setting

The ‘training’ data is defined here as Vampire data run at the constant dry adhesion level and is compared to the constant adhesion data runs performed at the wet, low and very low levels. These are compared in 5-second sections of moving time window data, the size of which was determined in this simulation as to be sensitive enough to identify changes.

Figure 7 demonstrates the clearly defined levels for the gain metric of the Sprague and Geers metric and that they are almost linearly decreasing with the corresponding reduction in adhesion level. Simple thresholds can therefore be set around these levels to determine the current adhesion level.

It should be noted that such high quality data at the lower adhesion levels may not be available in application. However the technique will give a clear indication that the adhesion level has varied for a particular section of track.

B. Step tests and signal delay

Vampire data was also created for a step change in the adhesion level from the dry condition to the very low at the half way point of the simulation at 30 seconds. The comparison to the ‘training’ data of the previous section is shown in Figure 7, which shows a clear reduction of the Sprague and Geers metric. Some time lag is evident due to the 5 second time windowing of the data, but this demonstrates that the technique can produce usable comparisons from signal based data alone.

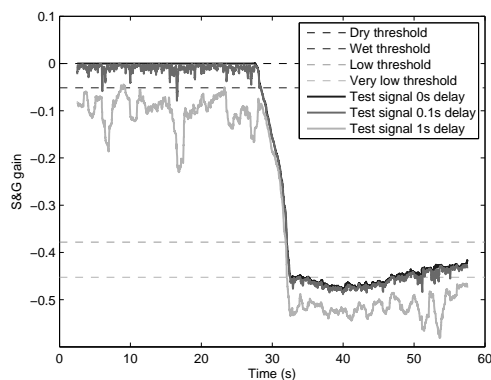


Fig. 7. Data comparison method adhesion threshold setting and step reduction tests at 30 seconds, for 0s time delay, 0.1s time delay and 1s time delay

The method will rely upon precise synchronisation of the ‘training’ and test data sets. The robustness of the algorithm was checked via delaying the ‘training’ data. This is also shown in Figure 7 for a 0.1 second and 1 second delay. The first case can be still seen clearly to demonstrate correlation though the quality is reduced. In the second case there is now a significant misalignment in the data, but the algorithm copes, not as clearly defining variations in adhesion but clearly demonstrating changes.

C. Fuzzy logic reasoning

Multiple signals offer the opportunity for more comparisons of the changes in the dynamics of the vehicle, once thresholds are set this essentially becomes a problem of data fusion. This can be accomplished through simple logic processes or more complex fuzzy logic reasoning the basic architecture of which is a current being developed.

V. CONCLUSION

Low adhesion causes punctuality and safety issues to rail operators and users alike due to vehicles failing to stop at stations or vehicles passing signals at danger. The RSSB managed project T959 is developing a number of practical processing options to determine the level of adhesion on in-service vehicles using relative modest cost sensors. The techniques’ efficacies are now being tested on more representative modelling data from the multi-bodies physics simulation package Vampire. To date the Kalman-Bucy filtering method of estimating creep forces has proven to work at the higher ends of the adhesion spectrum but fails to converge at the low adhesion levels, which is mostly likely due to a filter model mismatch and research is continuing to resolve the problem. A non-model based pragmatic data comparison method utilising the Sprague and Geers metric has so far proven positive in the estimation of low adhesion provided high quality comparison data is available and that any signal phase is within acceptable limits.

ACKNOWLEDGMENT

The authors would like to thank RSSB who manage project T959 with funding provided from the Rail Industry Strategic Research Programme. Thanks also goes to DeltaRail for the production of the Vampire simulation data.

REFERENCES

- [1] DeltaRail: Vampire software, <http://vampire-dynamics.com/>, accessed 11th April 2012
- [2] J. Kalker, On the rolling contact of two elastic bodies in the presence of dry friction, PhD Thesis, Delft University of Technology, Delft, Netherlands, (1967).
- [3] R. Kalman. A new approach to linear filtering and prediction, Transactions of the ASME Journal of Basic Engineering, volume 82 (series D), pp. 35-45, (1960).
- [4] L. Ljung, *System Identification: Theory for the User*, Prentice Hall, 1999.
- [5] T. Pearce and K. Rose, Measured force-creep relationships and their use in the vehicle response calculation, In proceedings of the 9th IAVSD symposium, Linkoping, (1985).
- [6] O. Polach, Creep forces in simulation of traction vehicles running on adhesion limit, *Wear*, volume 258(1), pp 992-1000, 2005.
- [7] RSSB: Research and development, <http://www.rssb.co.uk/RESEARCH/>, accessed 12th April 2012
- [8] L.E. Schwer, Validation metrics for response histories: perspectives and case studies, *Engineering with Computers*, 2007
- [9] C.P. Ward, R.M. Goodall and R.Dixon. Use of real time creep force estimation data for assessment of low adhesion in the wheel/rail contact, In proceedings of the The 5th IET conference on Railway Condition Monitoring and Non-Destructive Testing 29-30 November 2011, Derby Conference Centre(2011).
- [10] C.P.Ward, R.M.Goodall, R.Dixon, D.Fletcher, S.Lewis and G.Charles, RSSB Project T959 On-Board Detection of Low Adhesion, Interim Research Report, June 2011
- [11] A.H. Wickens. Fundamentals of rail vehicle dynamics, Guidance and Stability, Swets & Zeitlinger, Lisse, Netherlands, 2003